

## SYNTHESIS OF PLANT-MEDIATED SILVER NANOPARTICLES USING *CYPERUS DIFFORMIS* FLOWER EXTRACT AND EVALUATION OF ITS ANTIOXIDANT AND ANTICANCEROUS ACTIVITY

PANDURANG Y. PATIL<sup>1</sup>, GUNJAN S. KHAIRNAR<sup>1</sup>, SATISH B. MANJARE<sup>2</sup> AND VIJAY L. GURAV<sup>3</sup>

<sup>1</sup>Department of Environmental Science, Charitrakar Padma Bhushan Dr. Dhananjay Keer Ratnagiri Sub-Campus, University of Mumbai, P-61, MIDC, Mirjole, Ratnagiri 415 639, Maharashtra, India.

<sup>2</sup>Department of Chemistry, Charitrakar Padma Bhushan Dr. Dhananjay Keer Ratnagiri Sub-Campus, University of Mumbai, P-61, MIDC, Mirjole, Ratnagiri 415 639, Maharashtra, India.

<sup>3</sup>Department of Chemistry, Dapoli Urban Bank Senior Science College Dapoli, Dist-Ratnagiri 415 712, Maharashtra, India.

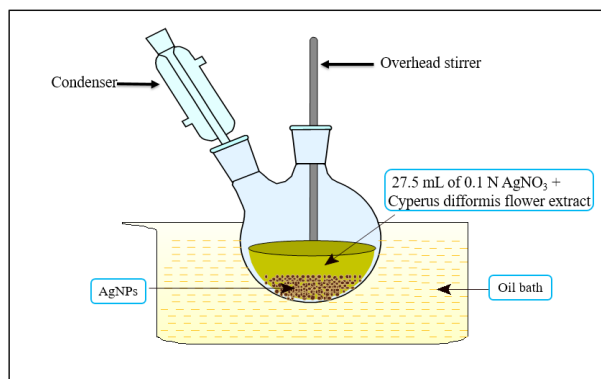
(Received 18 July, 2023; Accepted 2 September, 2023)

### ABSTRACT

Environment-friendly synthesis of silver nanoparticles is done by using *Cyperus difformis* flower extract. The AgNPs were synthesized by using a simple and cost-effective method. The synthesised AgNPs were characterized by using FTIR, XRD, FE-SEM/EDS, HR-TEM, ICP-AES and TGA. The HR-TEM shows particle size in the range of  $4.03965 \pm 215.32112$  nm- $54.42014 \pm 4.13582$  nm. The particle size of AgNPs by using HR-TEM analysis have good agreement with XRD analysis. These AgNPs show remarkable results for Anticancerous activity and antioxidant activity. The Anticancerous activity of biosynthesized AgNPs suggests their possible application in the medical industry.

**KEY WORDS :** AgNPs, *Cyperus difformis* flower extract, Antioxidant activity, Anticancerous activity

### GRAPHICAL ABSTRACT



### INTRODUCTION

Nowadays applicability of nanoparticles has great attention in the field of nanomedicines (Yohan and Chithrani, 2014) and catalysts (Manjare *et al.*, 2022).

### Abbreviations

AgNPs: Silver nanoparticles

AgNO<sub>3</sub>: Silver nitrate

nm: nanometer

mm: millimetre

FTIR: Fourier Transform Infrared Spectroscopy

XRD: X-Ray Diffraction

FE-SEM: Field Emission Scanning Electron Microscope

HR-TEM: High Resolution Transmission Electron Microscope

TGA: Thermo Gravimetric Analysis

DPPH: 1, 1-diphenyl-2-picryl-hydrazil

The nanoparticles usually are ranging from 1 nm to 100 nm (Manjare *et al.*, 2021). Nanoparticles have a high surface-to-volume ratio with smaller sizes. A specific surface area of nanoparticles enhances the catalytic reactivity (Sharma *et al.*, 2017) and other related activity such as antimicrobial activity

(Abdel-Aziz *et al.*, 2014) and antioxidant activity (Abdullah *et al.*, 2020) etc.

A lot of reviews are available on metal nanoparticles (MNPs) such as Pd (Manjare and Chaudhari, 2020a), (Manjare and Chaudhari, 2020b) and Ru (Pan *et al.*, 2001), (Gopinath *et al.*, 2014), Au (Rodríguez-león *et al.*, 2019) and Ag (Rautela *et al.*, 2019), (Herbin *et al.*, 2022) as a catalyst used in coupling reaction, oxidation and reduction reactions due to excellent activity and high specificity and good selectivity. Among the Nobel metals silver is one of the great choices due to its superior environment-friendly properties.

Generally, metal nanoparticles are produced by using either the physiochemical (Manjare *et al.*, 2020), (Abbas *et al.*, 2019), (Sreedhar, Surendra Reddy, and Keerthi Devi 2009) or green method (Shah *et al.*, 2021), (Gnanadesigan *et al.*, 2011), (Singhal *et al.*, 2011). The biosynthesis of AgNPs using extract of leaves of *Artocarpus heterophyllus* (Manjare, Paranjape, *et al.*, 2020) and *Carissa carandas* (Manjare, Sharma, *et al.*, 2020) has been reported.

In the present study, a flower extract of *Cyperus difformis* is used as a suitable source for the biosynthesis of AgNPs. To the best of our knowledge, there has been no report on the biosynthesis of AgNPs using *Cyperus difformis* as a stabilizing, capping-reducing agent.

## MATERIALS AND METHODS

All the chemicals were purchased from Hi Media, Ratnagiri, Maharashtra, India and used without purification. Solvents were dried by standard methods and is used for reactions *Cyperus difformis* flower were collected from Pawas, Dist-Ratnagiri, Maharashtra.

### Preparation of *Cyperus difformis* flower extract

In a 250 ml beaker, 10.0 gm of powder of *Cyperus difformis* flower was added to 100 ml of distilled water. This mixture was boiled for 15 minutes. Then this hot homogenous mixture was filtered through Whatman filter paper 1. This filtrate was cooled at room temperature and centrifuged at 2500 rpm for 10 minutes. The supernatant liquid was collected in a stoppered bottle. This liquid was stored in the refrigerator at 50 °C for further use.

### Synthesis of AgNPs from *Cyperus difformis* flower extract

The 10.0 ml of *Cyperus difformis* flower extract was

mixed with 27.5 ml of 0.1 N AgNO<sub>3</sub> solutions in 250 ml two necked round bottom flask. This homogenous mixture was kept in an oil bath attached to reflux condenser and it was stirred with the help of an overhead stirrer at 500 rpm at 90 °C temperature. The colour of the mixture was changed from colourless to brownish-black. This proves the formation of AgNPs. This stirred reaction mass was filtered through the Whatman filter paper 41. These fine AgNPs were dried in a hot air oven at a temperature 55±5 °C for 15 minutes.

### Antioxidant activity

The free radical activity of AgNPs was measured by using DPPH (1, 1-diphenyl-2-picryl-hydrazine) (Jadid *et al.*, 2017). The 2 mM of DPPH solution was prepared by taking 0.034 gm of DPPH (1, 1-diphenyl-2-picryl-hydrazine) into 50 ml methanol. The 2.0 ml of methanol and 1.0 ml of DPPH solution were mixed. In this mixture, the 50 microlitre AgNPs sample solution was added. This was kept in dark condition for 30 minutes. The absorbance was measured at wavelength 517 nm. Ascorbic acid was used as a standard. The radical scavenging assay was calculated by using the following formula-

Radical Scavenging Assay=

$$\frac{\text{Absorbance of control} - \text{Absorbance of sample}}{\text{Absorbance of control}} \times 100$$

The IC<sub>50</sub> values were calculated by using linear regression analysis and used to indicate the effectiveness of the antioxidant activity.

### Anticancerous Activity

The cytotoxicity of the AgNPs was assessed by using the human skin cancer cell line A375. The skin cancer cells were trypsinized and aspirated into 15 ml centrifuge tube. The cell count was adjusted using a DMEM medium. From this method, 10,000 cells were separated and incubated. Each cell plate is further incubated at 37 °C at a 5% CO<sub>2</sub> atmosphere for 24 hours. After 24 hours the skin cancer cell lines (A375) were aspirated. The different test concentrations (20, 40, 60, 80 and 100 µg/ml from stock). These plates were incubated at 37 °C and 5% CO<sub>2</sub> atmosphere for 24 hours. These plates were removed from the incubator and drug-containing media is aspirated. Then 10% MTT reagent is added in each well and further incubated at 37 °C and 5% CO<sub>2</sub> atmosphere for 3 hours. The culture medium was removed and then 100 µl of solubilisation

solution (DMSO) was added and further it was gently shaken in a gyratory shaker. The formazan is formed. The absorbance was measured by using a microreader at wavelengths 570 nm and 630 nm. The  $IC_{50}$  value was measured by using a dose-response curve for cell lines.

### Measurement and characterization

The FTIR (Fourier Transform Infrared) spectrum was acquired using the KBr pellet technique on a 3000 Hyperion microscope with vertex 80 FTIR system from Bruker, Germany. Bruker D2 Phaser diffractometer with Cu K $\alpha$  radiation ( $\lambda=1.5406$ ) was used to capture powder X-ray diffraction (PXRD) patterns. The diffraction pattern was observed in the range of 20-90° range. Field Emission-Scanning Electron Micrographs (FE-SEM) were obtained on a JSM-7600F microscope coupled with an EDX spectrometer. For the elemental analysis, energy dispersive X-ray spectroscopy (EDS) was utilised in conjunction with FE-SEM. HR-TEM analysis was performed with FEI, Tecnai G2, and F30 microscope. HR-TEM technique gives the size and morphology of nanoparticles. The inductively coupled plasma atomic emission spectrometer was used to find Ag content in AgNPs. This analysis was performed on SPECTRO Analytical Instruments GmbH, Germany. For ICP-AES analysis, AgNPs solution was dissolved in concentrated HNO<sub>3</sub> and concentrated H<sub>2</sub>SO<sub>4</sub> and then the Ag concentration of the solution was determined on the ICP-AES instrument.

## RESULTS AND DISCUSSION

### FTIR analysis

The functional groups present in the AgNPs were characterized by using FTIR. The FTIR spectrum is shown in Figure 1. The FTIR spectrum of AgNPs shows a strong absorbance at 3730.62 cm<sup>-1</sup> for stretching. The infrared band at 3441.36 cm<sup>-1</sup> for -OH stretching. The strong vibrations at 2918.52 cm<sup>-1</sup> to 2850.26 cm<sup>-1</sup> are due to the presence of -CH stretching frequency. The infrared bands at 1606.84 cm<sup>-1</sup> correspond to the C-N stretching of amine I bands of amines or aliphatic amines. The absorption peaks at 1577.35 cm<sup>-1</sup> and 1432.61 cm<sup>-1</sup> were characteristics of an amide bond. The structure of AgNPs was confirmed by -NH stretch, -OH stretch, -CH stretch, -CN stretch for alkaloids, terpenoids, flavonoids and proteins in the extract which acts as a reducing and stabilising agent.

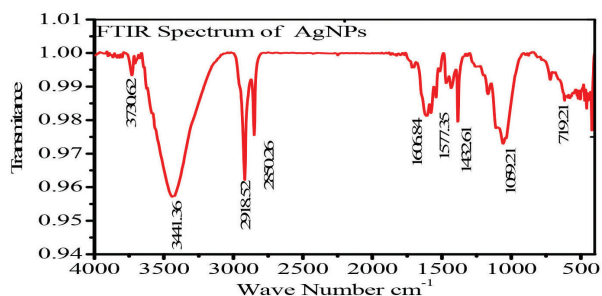


Fig. 1. FTIR spectrum of prepared AgNPs

### XRD analysis

The XRD spectrum of prepared AgNPs is shown in Figure 2. The powered XRD analysis was come out to examine the structure of AgNPs the distinct peaks of AgNPs were observed at 2 $\theta$  of 38.036, 46.082, 64.531, 76.838 (JCPDS file No.-04-0783) which demonstrated the crystallographic planes(III). Four unassigned peaks are marked with '#' were observed in the XRD spectrum of AgNPs. Theses peaks may be due to the crystallisation of bioorganic phase observed during the synthesis of AgNPs. The crystalline size of AgNPs determined by using

Scherrer formula:  $-D = \frac{K\lambda}{\beta \cos \theta}$ . The crystallite size of AgNPs is found that 1.3nm.

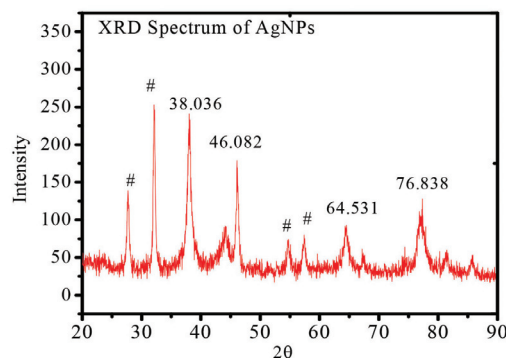


Fig. 2. X-ray diffraction pattern of AgNPs

### FE-SEM and EDS analysis

#### FE-SEM analysis

FE-SEM image of the sample are shown in Figure 3. The FE-SEM images shows flakes like morphology there is agglomeration of grains visible in FE-SEM images these flakes breaks into small particles having face centered cubic (FCC) in shape. EDS data of AgNPs is shown in Figure 4. EDS was use to find the elements present in the given sample. EDS data confirms the presence of elements K, Ag, Mg, Al, Fe and O.



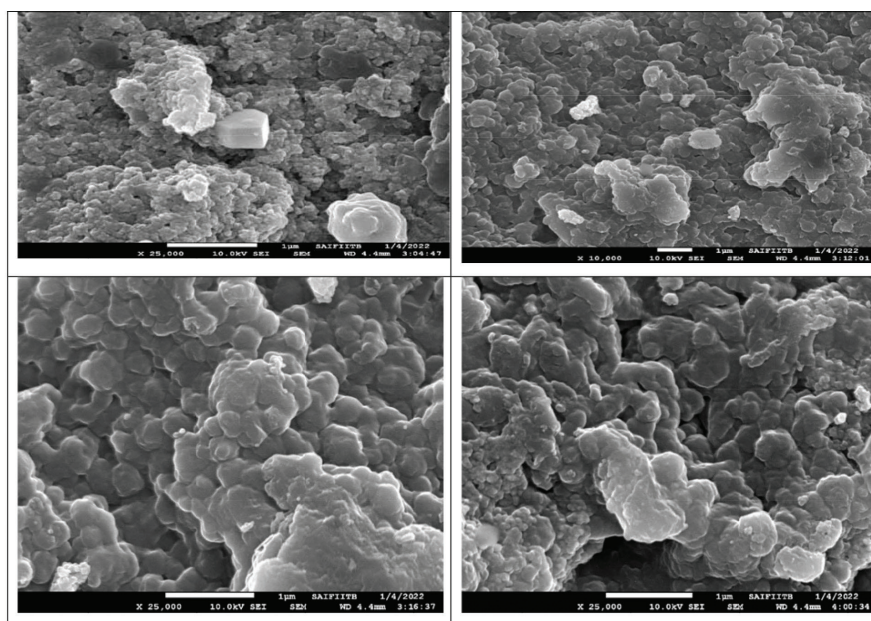


Fig. 3. FE-SEM analysis of prepared AgNPs

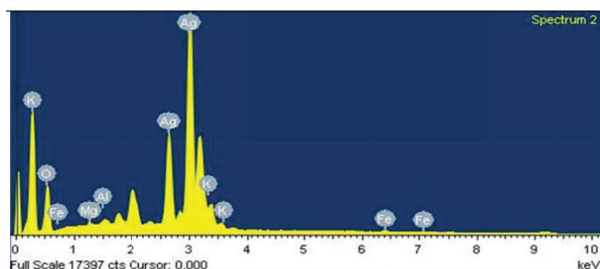


Fig. 4. EDS graph of prepared AgNPs

### HR-TEM Analysis

The high resolution transmission electron spectroscopy (HR-TEM) of AgNPs is shown in the Figure 5 [a), b),c) and d)]. The histogram of the particle size distribution shows average particle size distribution in the range of  $4.03965 \pm 215.32112$  nm- $54.42014 \pm 4.13582$  nm. The HR-TEM images show dark spot. These figures confirm the AgNPs are small sized. HR-TEM images shows that this AgNPs have a spherical in shape. This result of HR-TEM shows good agreement with XRD values.

### TGA analysis

TGA, DTA and DSC spectra have been recorded in temperature range from room temperature to 900 °C using simultaneous thermal system. The thermogravimetric analysis is carried out to find the thermal stability of AgNPs. A ceramic ( $Al_2O_3$ ) crucible was used for heating and measurements were carried out in air atmosphere at the heating rate of 10 °C/min. The TG- DSC graph of AgNPs is

shown in Figure 6a) and TG-DTA graph is shown in Figure 6b). This graphs shows that there is a no weight loss below 200 °C. The TGA plot of AgNPs exhibit that four step weight loss is observed upto 900 °C. The first weight loss observed is 10.14% at temperature 82.39 °C. This weight loss is for removal of physically adsorbed water on the surface of AgNPs (Khan *et al.*, 2011). The next minimal weight loss observed is 2.887% at 227.32 °C. This weight loss corresponds with removal of organic content. The third weight loss of 15.52% is observed at 475.21°C due to removal of inorganic content on the surface of AgNPs. The fourth step weight loss is observed at 600°C due to elimination of inorganic content. Finally, the 45.96% is the stable residue content of AgNPs. From TG-DSC graph Figure 6a), a sharp exothermic peak at 400 °C could be noted along with two small endothermic peaks, one at 500 °C and the other at 900 °C corresponding to the melting point of metallic silver (Kota *et al.*, 2017). From TG-DTA plot Figure 6b), displays an intense exothermic peak between 200 °C and 300 °C which are mainly attributed to crystallization of silver nanoparticles. According to this investigation, the synthesised AgNPs have good thermal stability up to 900 °C.

### ICP-AES analysis

The Ag content of AgNPs was calculated by using ICP-AES technique. The Ag content calculated by using ICP-AES in 500 mg is found to be 205 mg. This result shows good ion porosity for prepared AgNPs.

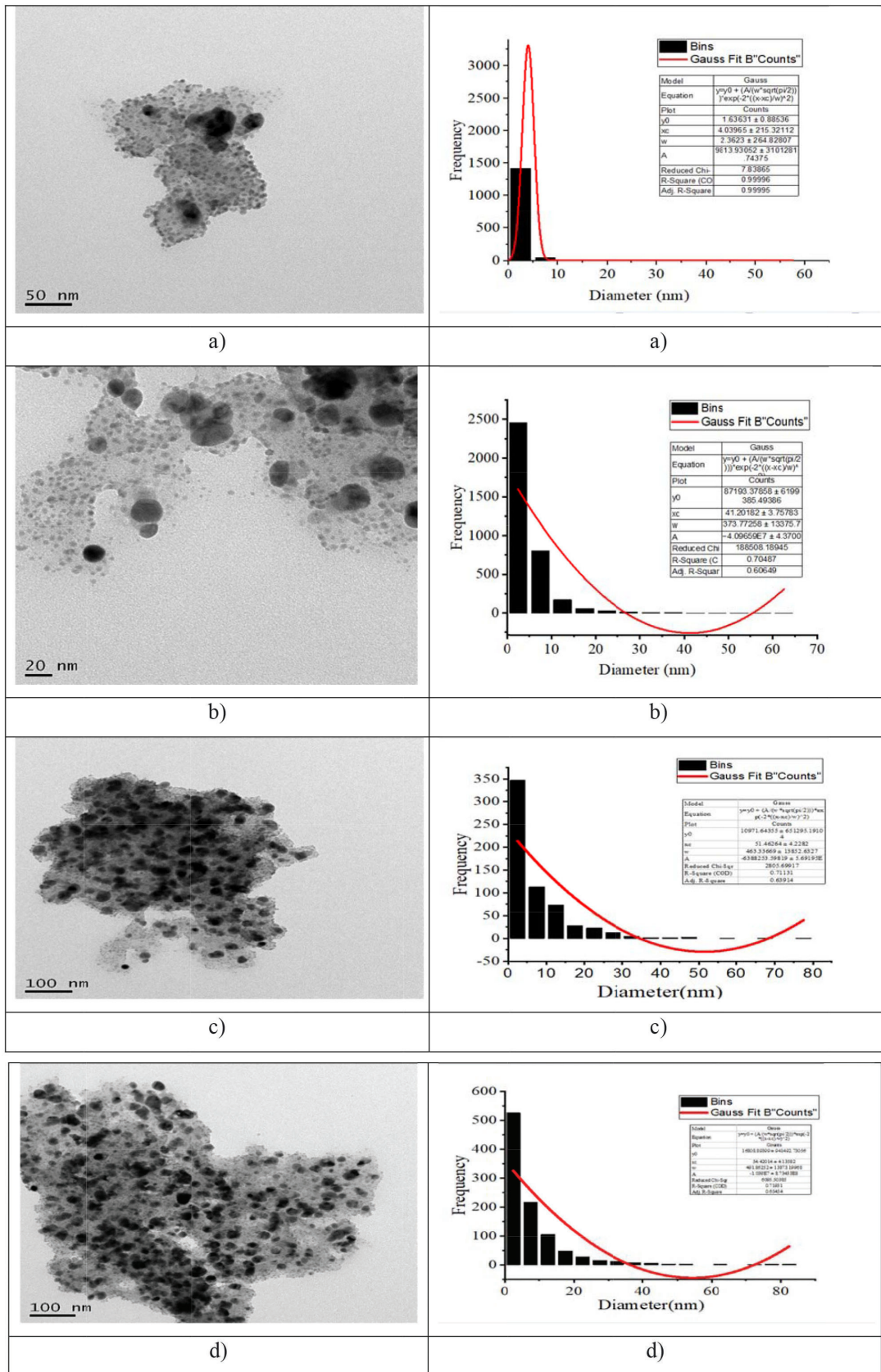


Fig. 5. HR-TEM analysis and particle size distribution of distribution of AgNPs [a), b), c) and d)]



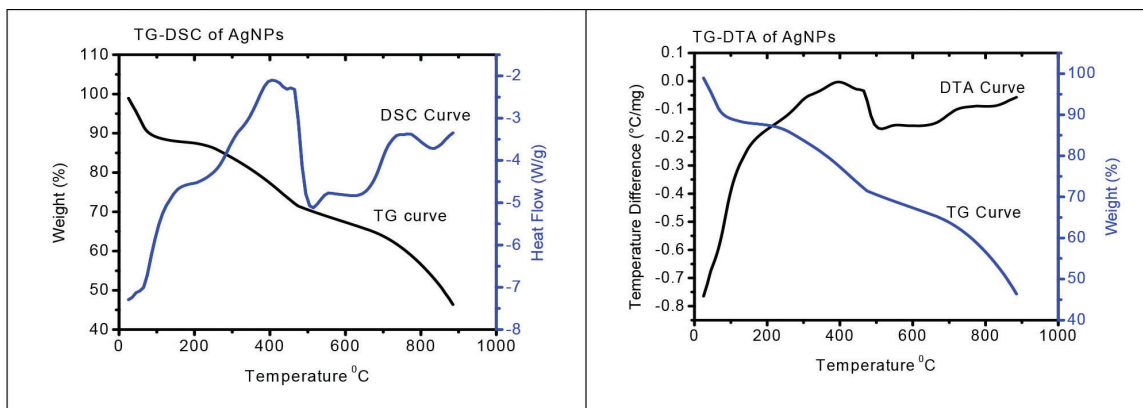


Fig. 6. a) TG-DSC analysis of prepared AgNPs

Fig. 6. b) TG-DTA analysis of prepared AgNPs

### Antioxidant activity

The lower the  $IC_{50}$  value the higher is the antioxidant activity of testing sample (Jadid *et al.* 2017). The significant antioxidant potential was measured by DPPH (1, 1-diphenyl-2-picryl-hydrazil) as a radical scavenging capacity. The antioxidant activity observed for AgNPs is  $IC_{50}=58.45 \mu\text{g/ml}$ . This shows significant activity for prepared AgNPs. The DPPH assay graph is as shown in Figure 7.

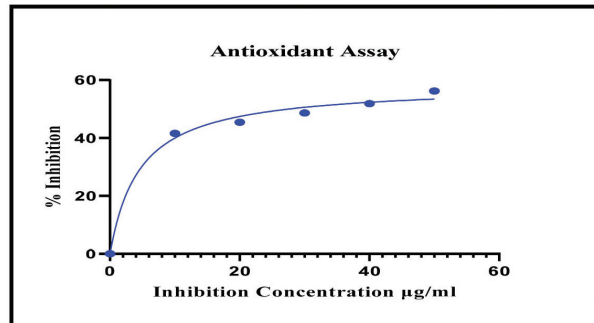


Fig. 7. DPPH assay graph of prepared AgNPs

### Anticancerous activity

The cytotoxicity activity of AgNPs was tested against the skin cancer celllines ( $A_{375}$ ). The dose response curve is shown in Figure 8 [a] and b]. The results obtained for  $A_{375}$  celllines after 24 hours reflects a  $IC_{50}$  is  $66.15 \mu\text{g/ml}$ . The AgNPs dose for  $A_{375}$  celllines is more pronounced and effective.

### CONCLUSION

The AgNPs were synthesized by using environment-friendly and easy step. The AgNPs was successfully prepared by using *Cyperus difformis* flower extract as a reducing and stabilizing agent. It is observed that the AgNPs yield is good (80%). The FTIR analysis confirms that the groups present in alkaloid and terpenoids. These groups act as a reducing agent for synthesis of AgNPs. The synthesized AgNPs shows good antioxidant property with  $IC_{50}=58.45 \mu\text{g/ml}$ . The AgNPs dose for skin cancer celllines shows remarkable results with  $IC_{50}$  value as  $66.15 \mu\text{g/ml}$ . As a result of these

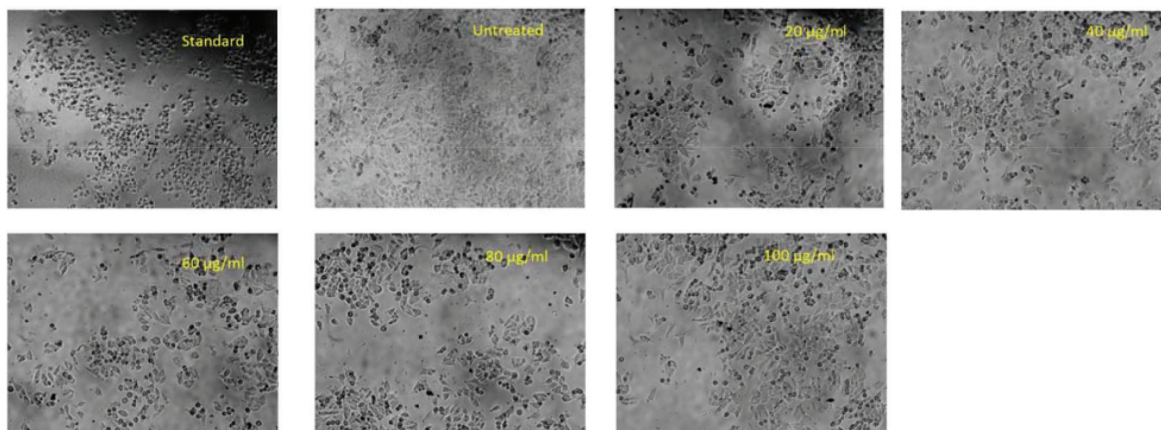


Fig. 8a). (a) Cytotoxicity of AgNPs against human Skin cancer cell line A-371

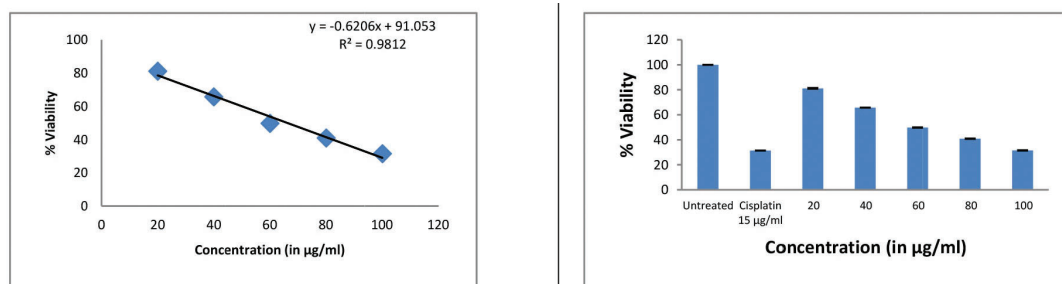


Fig. 8b). Percentage of cell inhibition in human Skin cancer cell line A-371 with different concentrations

findings, it is possible to cure skin cancer with AgNPs derived from *Cyperus difformis* flower extract.

**Author Contribution:** All of the authors have taken full responsibility for the content of this manuscript.

**Funding:** No funding was received.

**Data Availability:** My manuscript and associated personal data will be shared with Research Square for the delivery of the author dashboard.

**Declarations:** The authors declare that they have no conflict of interest. The authors declare that they have no known competing financial interests or personal relationships that could have appeared to influence the work reported in this research paper.

**Informed consent:** The authors consent to participate.

**Consent for publication:** The author's consent for publication.

## REFERENCES

- Abbas, G., Kumar, N., Kumar, D. and Pandey, G. 2019. Effect of Reaction Temperature on Shape Evolution of Palladium Nanoparticles and their Cytotoxicity against A 549 Lung Cancer Cells. *ACS Omega*. 4: 21839-47. <https://doi.org/10.1021/acsomega.9b02776>.
- Abdel-Aziz, M. S., Shaheen, M.S., El-Nekeety, A.A. and Abdel-Wahhab, M.A. 2014. Antioxidant and Antibacterial Activity of Silver Nanoparticles Biosynthesized Using *Chenopodium Murale* Leaf Extract. *Journal of Saudi Chemical Society*. 18 (4): 356-363. <https://doi.org/10.1016/j.jscs.2013.09.011>.
- Abdullah, J. A.A., Eddine, L. S., Abderrhmane, B., Alonso-González, M., Guerrero, A. and Romero, A. 2020. Green Synthesis and Characterization of Iron Oxide Nanoparticles by *Pheonix Dactylifera* Leaf Extract and Evaluation of Their Antioxidant Activity. *Sustainable Chemistry and Pharmacy*. 17 (April). <https://doi.org/10.1016/j.scp.2020.100280>.
- Gnanadesigan, M., Anand, M., Ravikumar, S., Maruthupandy, M., Vijayakumar, V., Selvam, S., Dhineshkumar, M. and Kumaraguru, A.K. 2011. Biosynthesis of Silver Nanoparticles by Using Mangrove Plant Extract and Their Potential Mosquito Larvicidal Property. *Asian Pacific Journal of Tropical Medicine*. 4 (10): 799-803. [https://doi.org/10.1016/S1995-7645\(11\)60197-1](https://doi.org/10.1016/S1995-7645(11)60197-1).
- Gopinath, K., Karthika, V., Gowri, S., Senthilkumar, V., Kumaresan, S. and Arumugam, A. 2014. Antibacterial Activity of Ruthenium Nanoparticles Synthesized Using *Gloriosa superba* L. Leaf Extract. *Journal of Nanostructure in Chemistry*. 4 (1): 4-9. <https://doi.org/10.1007/s40097-014-0083-4>.
- Herbin, H. B., Aravind, M., Amalanathan, M., Sony Michael Mary, M., Lenin, M. M., Parvathiraja, C., Siddiqui, M. R., Wabaidur, S. M. and Islam, A. 2022. Synthesis of Silver Nanoparticles Using *Syzygium Malaccense* Fruit Extract and Evaluation of Their Catalytic Activity and Antibacterial Properties. *Journal of Inorganic and Organometallic Polymers and Materials*. 1-14.
- Jadid, N., Hidayati, D., Hartanti, S. R., Arraniry, B. A., Rachman, R. Y. and Wikanta, W. 2017. Antioxidant Activities of Different Solvent Extracts of *Piper Retrofractum* Vahl. Using DPPH Assay. *AIP Conference Proceedings*. 1854 (June 2017). <https://doi.org/10.1063/1.4985410>.
- Khan, M. A. M., Kumar, S., Ahamed, M., Alrokayan, S. A and AlSalhi, M. S. 2011. Structural and Thermal Studies of Silver Nanoparticles and Electrical Transport Study of Their Thin Films. *Nanoscale Research Letters*. 6 (1): 1-8. <https://doi.org/10.1186/1556-276X-6-434>.
- Kota, S., Dumpala, P., Anantha, R. K., Verma, M. K. and Kandepu, S. 2017. Evaluation of Therapeutic Potential of the Silver/Silver Chloride Nanoparticles Synthesized with the Aqueous Leaf Extract of *Rumex acetosa*. *Scientific Reports*. 7 (1): 1-11. <https://doi.org/10.1038/s41598-017-11853-2>.
- Manjare, S. B. and Chaudhari, R. A. 2020a. Environment-Friendly Synthesis of Palladium Nanoparticles Loaded on Zeolite Type-Y (Na-Form) Using *Anacardium occidentale* Shell Extract (Cashew Nut Shell Extract), Characterization and Application in C-C Coupling Reaction. *Journal of Environmental*

- Chemical Engineering*. 8 (5): 104213. <https://doi.org/10.1016/j.jece.2020.104213>.
- Manjare, S. B., Chaudhari, R. A., Thopate, S. R., Risbud, K. P. and Badade, S. M. 2020. Resin Loaded Palladium Nanoparticle Catalyst, Characterization and Application in -C-C- Coupling Reaction. *SN Applied Sciences*. 2 (5): 1-6. <https://doi.org/10.1007/s42452-020-2795-z>.
- Manjare, S. B., Paranjape, P. P., Gurav, V. L., Shinde, P. P., Chavan, R. R. and Thopate, S. R. 2020. Silver Nanoparticles Synthesis Using AH Leaf Extract and Its Antimicrobial Activity. *Bioinspired, Biomimetic and Nanobiomaterials*. 9 (3): 190-193. <https://doi.org/10.1680/jbibn.19.00047>.
- Manjare, S. B., Pendhari, P. D., Badade, S. M. and Thopate, S. R. 2021. Palladium Nanoparticles: Plant Aided Biosynthesis, Characterization, Applications. *Chemistry Africa*. 4 (4): 715-730. <https://doi.org/10.1007/s42250-021-00284-2>.
- Manjare, S. B. and Chaudhari, R. A. 2020b. Palladium Nanoparticle Bentonite Hybrid Using Leaves of Syzygium Aqueum Plant from India/: Design and Assessment in the Catalysis of -C-C-Coupling Reaction. *Chemistry Africa*. no. 0123456789. <https://doi.org/10.1007/s42250-020-00139-2>.
- Manjare, S. B., Pendhari, P. D., Badade, S. M., Thopate, S. R. and Thopate, M. S. 2022. Biosynthesis of Palladium Nanoparticles from *Moringa oleifera* Leaf Extract Supported on Activated Bentonite Clay and Its Efficacy Towards Suzuki-Miyaura Coupling and Oxidation Reaction. *Bio Nano Science*. 12 (3): 785-794. <https://doi.org/10.1007/s12668-022-01011-y>.
- Manjare, S. B., Sharma, S. G., Gurav, V. L., Kunde, M. R. and Patil, S.S. 2020. Biosynthesis of Silver Nanoparticles Using Leaf and Bark Extract of Indian Plant *Carissa carandas*, Characterization and Antimicrobial Activity. *Asian Journal of Nanoscience and Materials*. 3: 58-66. <https://doi.org/10.26655/AJNANOMAT.2020.1.6>.
- Pan, C., Pelzer, K., Philippot, K., Chaudret, B., Dassenoy, F. Lecante, P. and Casanove, M. 2001. Ligand-Stabilized Ruthenium Nanoparticles/: Synthesis , Organization , and Dynamics. *Journal of American Chemical Society*. 123 (31): 7584-7593.
- Rautela, A., Rani, J. and Debnath (Das), M. 2019. Green Synthesis of Silver Nanoparticles from Tectona Grandis Seeds Extract: Characterization and Mechanism of Antimicrobial Action on Different Microorganisms. *Journal of Analytical Science and Technology*. 10 (1): 1-10. <https://doi.org/10.1186/s40543-018-0163-z>.
- Rodríguez-león, E., Rodríguez-vázquez, B.E., Martínez-higuera, A., Rodríguez-beas, C., Larios-rodríguez, E., Navarro, R.E., López-esparza, R. and Iñiguez-palomares, R.A. 2019. Synthesis of Gold Nanoparticles Using *Mimosa tenuiflora* Extract, Assessments of Cytotoxicity, Cellular Uptake, and Catalysis. *Nanoscale Rese*. 14: 1-16.
- Shah, M.Z., Guan,Z., Din, A.U., Ali, A., Rehman, A.U., Jan, K., Faisal, S., Saud, S., Adnan, M., Wahid, F., Almari, S., Siddiqui, M. H., Ali, S., Nasim, W., Hammad, H. M. and Fahad, S. 2021. Synthesis of Silver Nanoparticles Using *Plantago lanceolata* Extract and Assessing Their Antibacterial and Antioxidant Activities. *Scientific Reports*. 11 (1): 1-14. <https://doi.org/10.1038/s41598-021-00296-5>.
- Sharma, M., Sarma, P. J., Goswami, M. and Bania, K.K. 2017. Metallogel Templated Synthesis and Stabilization of Silver-Particles and Its Application in Catalytic Reduction of Nitro-Arene. *Journal of Colloid and Interface Science*. 490: 529-541. <https://doi.org/10.1016/j.jcis.2016.11.065>.
- Singhal, G., Bhavesh, R., Kasariya, K., Sharma, A.R. and Singh, R.P. 2011. Biosynthesis of Silver Nanoparticles Using *Ocimum sanctum* (Tulsi) Leaf Extract and Screening Its Antimicrobial Activity. *Journal of Nanoparticle Research*. 13 (7): 2981-2988. <https://doi.org/10.1007/s11051-010-0193-y>.
- Sreedhar, B., Reddy, R.S. and Devi, K. 2009. Direct One-Pot Reductive Amination of Aldehydes with Nitroarenes in a Domino Fashion: Catalysis by Gum-Acacia-Stabilized Palladium Nanoparticles. *Journal of Organic Chemistry*. 74 (22): 8806-8809. <https://doi.org/10.1021/jo901787t>.
- Yohan, D. and Chithrani, B.D. 2014. Applications of Nanoparticles in Nanomedicine. *Journal of Biomedical Nanotechnology*. 10 (9): 2371-2392. <https://doi.org/10.1166/jbn.2014.2015>.
-